Nanoscale morphology of lignins and their chemical transformation products

SERGEY M. SHEVCHENKO, GEORGE W. BAILEY, Y. SHANE YU, AND LEONID G. AKIM

ABSTRACT

Reductive splitting experiments demonstrated a high degree of preservation of typical lignin structures in humic substances that are the major products of lignin environmental biodegradation.Atomic force microscopy and scanning tunneling microscopy provided a comparative analysis of the morphological character of lignin,lignin model compounds, and humic substances sorbed on organic and mineral surfaces. Chemical and morphological similarity between lignins and humic substances suggests the use of waste lignins as soil improvement agents.

Application

The fundamental information in this paper will help develop new uses for waste lignins as soil improvement agents in agriculture and forestry.

ULTRASTRUCTURE AND SURFACE morphology influence the behavior of wood and its constituents in technological and environmental processes *(1, 2)*. The last decade has seen the introduction of new experimental tools for studying surface morphology of natural materials.Such means include atomic force microscopy (AFM) and scanning tunneling microscopy (STM) *(3–5)*. These are also promising methods to study wood and pulping chemistry. In addition,they may provide better resolution and higher versatility in sample preparation.

The techniques have only had limited application with wood-related samples to date *(6–8)*. This study therefore applied AFM and STM to a series of lignins, their model compounds, and humic substances. The humic substances are the same products of the biotransformation of wood litter in the environment *(9–11)*.

For many years, electron microscopy was the only method providing micrometer-scale surface images of wood constituents *(2)*. Researchers applied that technique to pulping lignins *(12–15)*, milled wood lignins *(13–18)*, lignin-polysaccharide complexes *(17, 18)*, and soil humic substances *(19)*. Some investigators studied lignin model compounds using X-ray crystallography *(20, 21)*. These compounds also happen to be the typical components of lignin degradation under pulping and environmental conditions. The studies did not provide information on surface properties or the relationship with electron microscope images of amorphous polymers, however. This paper therefore pursues a unified approach to all classes of lignin-related compounds.

One must consider both the theoretical and applied viewpoints when comparing the surface morphology of model compounds, wood lignin, pulping lignins, and humic substances.Lignin modeling is a controversial topic. The properties of native lignin that oligomeric models and model dehydrogenation polymers can simulate are still unclear. For morphology of lignin, there are no experimental data to confirm its structure. In addition, changes in morphology during the chemical transformation of lignin into oligomeric degradation products, pulping lignins, and humic substances may affect chemical structure and properties.

Oligomeric degradation products of lignin may behave as aggregates in the environment.The surface characteristics of organic constituents may interact with the complexing and chelating characteristics of soil. There will also be an influence from the ability of the soil to bind environmental pollutants such as heavy metal cations.

Similarities and differences between humic substances and lignins are of special interest. Oxygenation of lignins during industrial processes is chemically similar to their oxidation in the environment *(9, 22)*. Nontoxic, high molecular weight pulping wastes could form humus in soil to improve soil for agriculture and forest uses. Transformation mechanisms similar to natural humification might also provide specific degradative pathways for new industrial plastics containing lignin-related structural blocks. Incorporation of transformed anthropogenic polymers into the organic matter of soil through composting could offer a faster, cheaper, and easier disposal technology to industries interested in recycling and the development of environmentally friendly products. Comparison of the surface properties of native lignins,pulping lignins, and humic substances is a necessary step in this direction.

One might also expect that solid inorganic constituents in soil and coating agents in paper strongly interact with highly hydroxylated polar macromolecules derived from lignin after biodegradation (humic and fulvic acids) or pulping (residual

Image	d_f
2 a.	2.23
2 b.	2.26
2 c.	2.17
2 d.	2.22
2 e.	2.07
2 f.(3 b.)	2.21
2 g.(3 e.)	2.34
4 b.	2.17
4 d.	2.19
6 c.	2.10
6 f.	2.23
8 e.	2.12
9 b.	2.15

I. Fractal dimensions, df, for nanometer-scale images

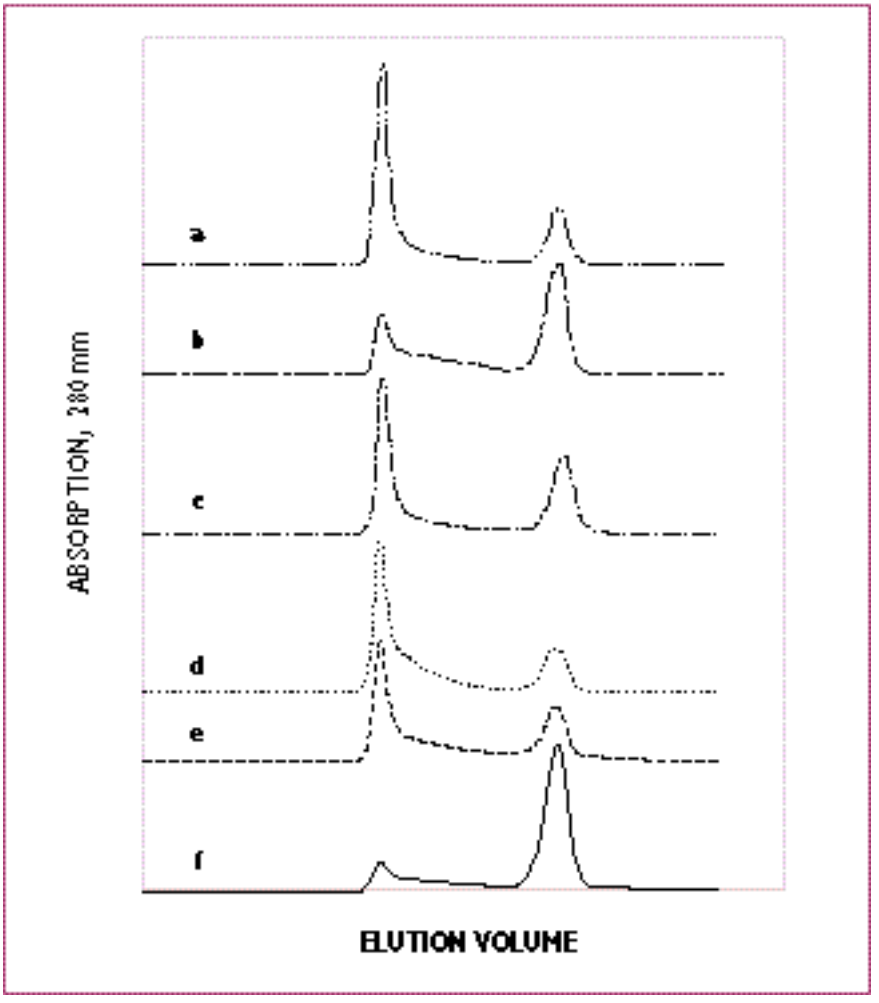

1. Gel permeation chromatograms:a. peat humic acid, b. Suwannee River fulvic acid, c. Suwannee River humic acid, d. Canadian soil fulvic acid, e. commercial humic acid, and f. birch milled wood lignin treated with dry hydrogen iodide in $CHCl_3$

lignin). Evaluation of the effect of such interactions on the surface morphology of these polymers presents a special problem of scientific and applied interest.

EXPERIMENTAL

Sample preparation

We obtained milled wood lignins from birch and spruce and dioxane lignin from eucalyptus according to standard procedures *(23, 24)*. The samples of pulping lignins used were lignin from oxygen-acetone pulping *(25)* and commercial,sugar-free spruce sodium lignosulfonate. Coniferyl alcohol "end-wise" dehydrogenation polymer (DHP) *(26)* came from J.F.D. Dean and K.-E. L. Eriksson.The source of lignin model compounds was Aldrich Co. We synthesized 1-(4-hydroxyphenyl)-2-(2-methoxyphenoxy) ethanol as described earlier *(20)*. Reductive depolymerization experiments used the following samples of humic substances: soil fulvic acid purchased from Concordia University, commercial humic acid from Fluka AG, standard Suwannee River fulvic acid, Suwannee River humic acid, and peat humic acid from the International Humic Substances Society. The ATM experiments also used standard Suwannee River fulvic and humic acids and Canadian soil fulvic acid. Indian muscovite came from WARDs. Union Carbide Corp. provided the highly oriented pyrolytic graphite. The work used deionized water filtered through a commercial water purification system with the quality greater than 18 ohm^{-1}. We also used a commercial dryer.

We cleaved a graphite surface using a small piece of transparent adhesive tape. Preparation of the muscovite substrate involved cutting a 1 x 1 cm piece of freshly cleaved Indian muscovite. We mounted the flake on the AFM glue-coated, metal sample puck. We stored prepared substrates in a small desiccator-containing dryer until used. We transferred 5 µL of a sample solution (50 mg/L) to the substrate surface. After drying for 2 h at room conditions, we placed the sample on the stage and scanned it at room temperature and atmospheric conditions. We calculated fractal dimensions and structural characteristics of imaged surfaces using a computer program.

Treatment of samples with HI

For the ^1H NMR check, we suspended the samples in $CDCl_3$ (1 mg in 1.5 mL).The reaction vessels were 5 mm OD NMR tubes. We bubbled

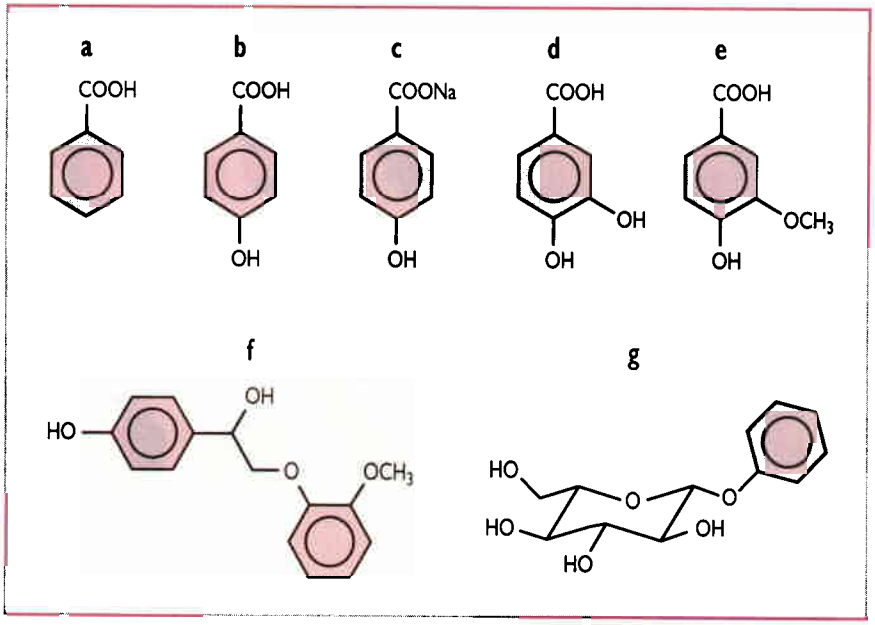

2. Model compounds studied by atomic force microscopy: a. Benzoic acid, b. 4-hydroxybenzoic acid, c. sodium 4-hydroxybenzoate, d. 3,4-dihydroxybenzoic acid, e. 4-hydroxy-3-methoxy-benzoic acid, f. 1-(4-hydroxyphenyl)-2-(2-methoxyphenoxy) ethanol, and g. phenyl-β-D-glucopyranoside

dry HI with nitrogen flow through the suspension for 1.5 h. We recorded the ^{1}H NMR spectra of the reaction mixture every 20 min with an external standard. In the gel permeation chromatographic (GPC) analyses, we bubbled dry HI with nitrogen flow through the sample suspended in $CHCl_3$ (1 mg in 1.5 mL). After 1.5 hours, we filtered the insoluble polymer, washed with dry chloroform, and then dried *in vacuo*. Since chloroform would only remove monomeric product, we completely dissolved the entire sample of the treated polymer in dimethylsulfoxide (DMSO) before the GPC analysis. We recorded the Fourier transform ^{1}H NMR spectra with a Bruker AC-200 instrument. GPC came from a Sephadex LH-20 (fine) with a 870 x 10 mm column. DMSO with 0.03*M* H_3PO_4 and 0.03*M* LiBr was the eluent at a rate of 1 mL/min. UV light at a wavelength of 280 nm monitored the chromatograms.

Scanning probe microscopy

This study used a NanoScope III scanning probe microscope. A scanning tunneling microscope and an atomic force microscope are components of the scanning probe microscope system. The STM device had a Pt-Ir tip (0.64-cm length, 0.03-cm diameter) fitted with a 12-μm scan head. Before instrument engagement, we adjusted the tip-surface distance to approximately 0.1 mm by lowering the scan head. Each atomic force microscope silicon tip has a sharp edge whose surface reflects the laser beam. The tips are very soft and can bend. Each tip has a force constant of 0.6 Newton/m. We optimized the operational parameters during the real-time scans.

Computer-assisted reconstruction

The calculations used SYBYL software on a Silicon Graphics IRIS Indigo R4000 Elan workstation. The molecular mechanics conformational calculations used the Tripos force field *(27)* to accomplish full geometry optimization. The Gasteiger-Hückel method calculated the atomic charges. In this, we determined the σ-components according to Gasteiger and Marsili *(28)* and the π-components by the standard Hückel method *(29)*. The total charge was the sum of σ and π charges. The simulated graphite substrate planes remained "frozen" during all optimizations. We applied the docking procedure to simulate the behavior of aggregates and macromolecules on the surface and then optimized the structures. The figures discussed later do not show graphite planes. Geometrical parameters of the lignin model compound, 1-(4-hydroxyphenyl)-2-(2-methoxyph noxy) ethanol, are from X-ray crystallographic data *(20)*. In simulation of lignin chains, erythro-all-RS-guaiacyl and syringyl chains used construction with initial geometry parameters of dimeric structures *(21, 30)*. The simulation also used an alternative, more extended conformer. This material has 0.3 kcal/mole higher energy when using the Tripos force field. It may be the lowest energy conformer when using another force field *(31)*. Construction of the β-D-glucopyranoside chain simulated a carbohydrate using standard geometry parameters from the SYBYL software. In the simulation, the graphite surface had almost no effect on the spatial organization of the lignin and carbohydrate model polymers. Calculations of molecular dynamics on the polymeric chains used the simulated annealing technique followed by full optimization of the conformers. We shall publish details of the computations elsewhere.

RESULTS

Relationships between plant lignins and soil humic substances are still a controversial topic *(9)*. Before conducting microscopical experiments,

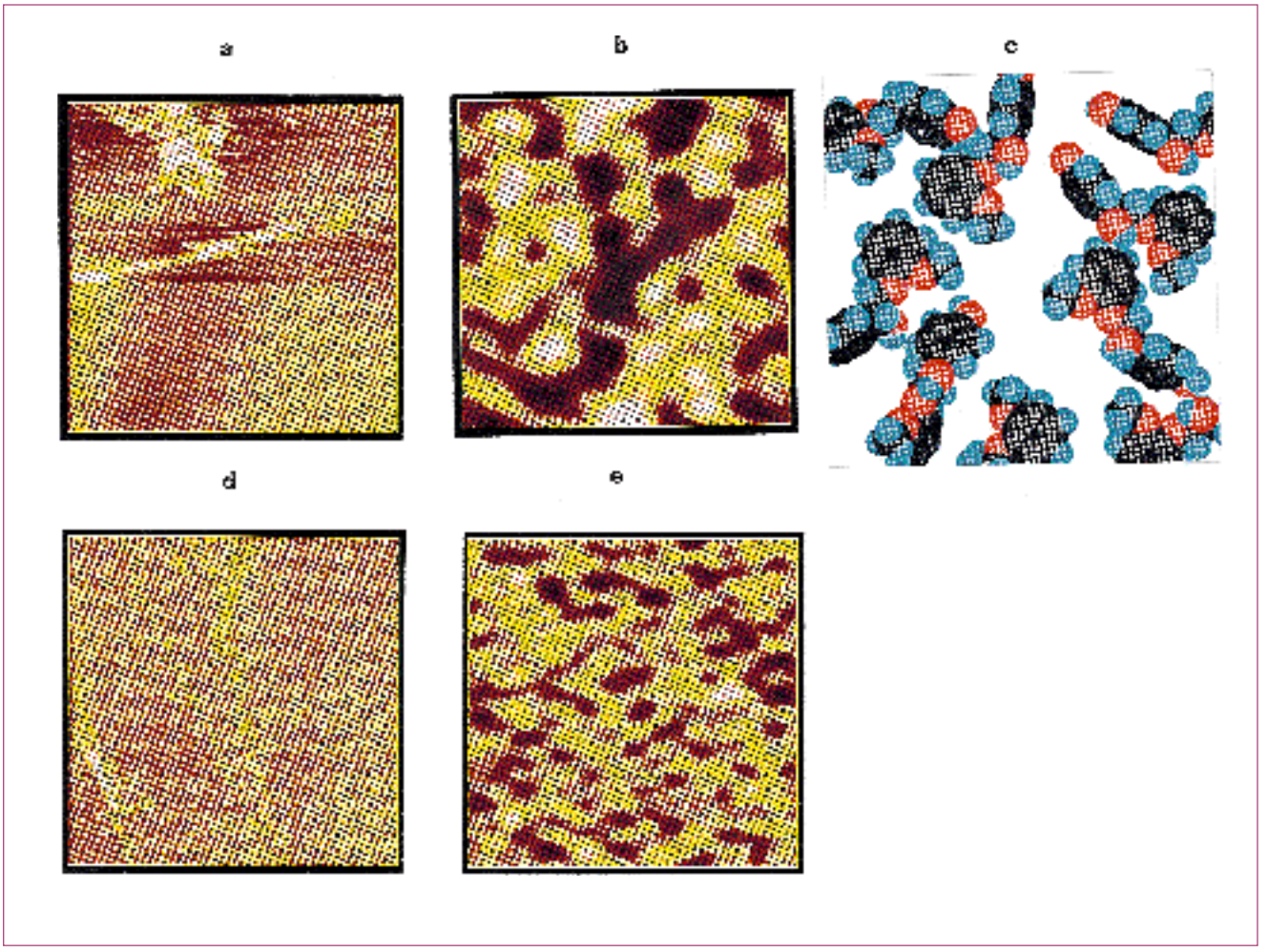

3. AFM images of model compounds on graphite for 1-(4-hydroxyphenyl)-2-(2- methoxyphenoxy)ethanol (Fig. 2 f.) deposited from acetone:a. 6 x 6 µm, height 0–60 nm; b. 2.5 x 2.5 nm, height 0–0.6 nm; c. computer reconstruction of molecular aggregate corresponding to image b. with the same scale and phenyl-ß-D-glucopyranoside (Fig. 2 g.) deposited from dioxane:d. 6 x 6 µm, height 0–60 nm; e. 2.5 x 2.5 nm, height 0–1.5 nm

we therefore wanted to provide more chemical data proving the theory of preservation of major features of lignin structure in humic substances. We recently developed a powerful technique of ultra-mild splitting of lignin with hydrogen iodide *(32, 33)*. In this procedure, lignin and its model dehydrogenation polymers yield as major products monolignol diiodide and a mixture of trimeric structures produced from linear blocks and branching knots in lignin structure, respectively *(34)*. The same procedure applied to aquatic and soil fulvic acids, humic acids, and peat gave no noticeable level of any monomeric products. **Figure 1** shows that GPC of humic substances were very similar to those of wood lignin,however. This reveals a significant amount of splittable, lignin-inherited trimeric blocks in humic substances.

The AFM technique produced images of irregular aggregates of solid lignin model compounds (**Fig. 2**) formed on graphite after drying from a dilute solution. We expected fast drying to yield nonequilibrium aggregates characterized by a random morphology different from a regular crystal. **Table I** reveals that all the images have a similar morphology characterized by the same fractal dimension values *(35)*. **Figure 3** gives some examples. In nanometer-scale surfaces, individual molecules and functional groups were evident. This figure also presents computer-assisted reconstruction of possible spatial organization of individual molecules in a random aggregate.

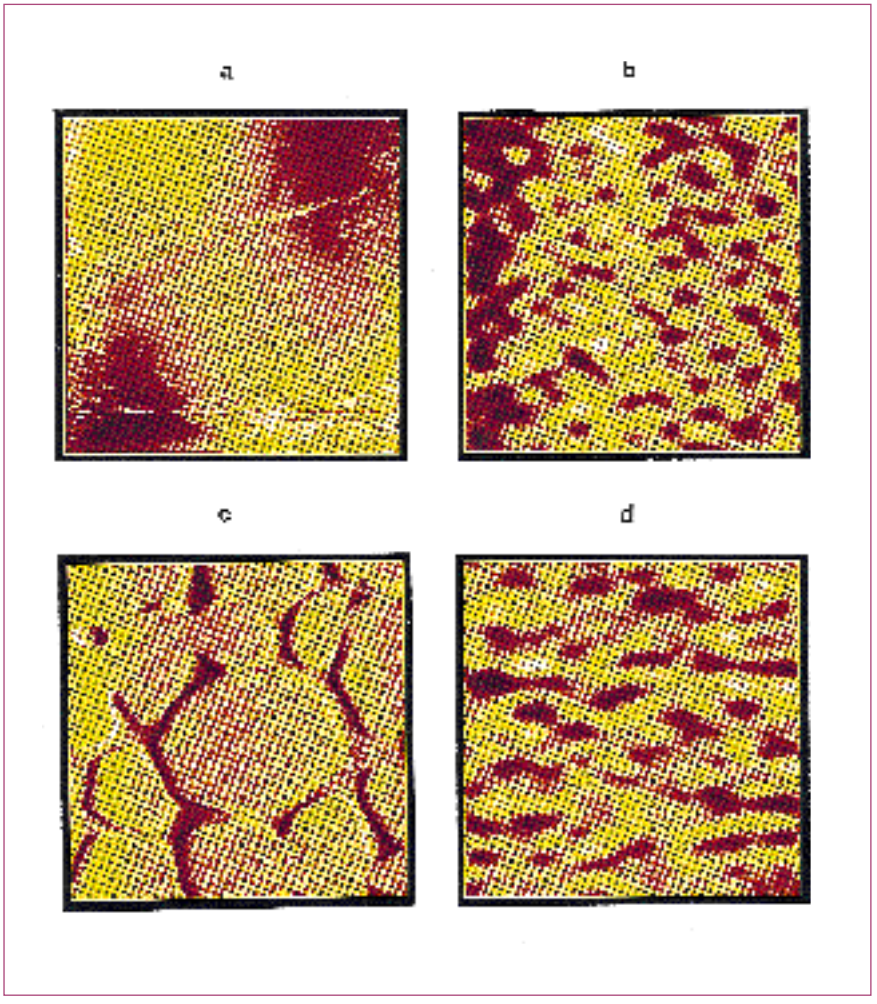

4. AFM images of dehydrogenation polymer of coniferyl alcohol deposited from dioxane on graphite: a. 10 x 10 μm, height 0–47 nm; b. 2 x 2 nm, height 0–0.5 nm and muscovite; c. 5 x 5 μm, height 0–25 nm; d. 3.5 x 3.5 nm, height 0–1 nm

Figure 4 shows that amorphous "end-wise" DHP of coniferyl alcohol also gave images of high quality on graphite and muscovite. The chemical nature of the substrate surface obviously influenced the morphology of the polymer aggregates at the micrometer scale. The cross-section analysis proved that the nanometer morphology of the model polymer is similar on the two substrates, however. It is also similar to low molecular weight lignin model compounds. (Compare fractal dimension values for images 3a, 3e, 4b, and 4d.) Our observations do not confirm an earlier report on surprisingly regular STM images of DHP *(8)* that probably resulted from an artifact.

The surface morphology of spruce in **Fig. 5** and birch in **Fig. 6** milled wood lignins is also substrate sensitive. We could achieve nanometer-scale resolution for birch and eucalyptus lignins. The nanometer-scale images revealed filamentous structures that may be the chain fragments in a lignin network. Computer simulations suggest a possibility of two major types of regular tertiary organization of lignin chains—an extended helix and a flexible helix. **Figure 7** shows the ribbon-like structure characteristic of carbohydrates. Molecular dynamics simulations followed by full geometry optimization have revealed sterically unstrained, irregular conformers. These may contain some regular structures of a broad, flattened helix type shown in Fig. 7. Comparing Figs.6c and 7c shows that they may be the best approximations of the filaments on the experimental image of birch lignin. A better approximation of the experimental image of eucalyptus lignin probably comes from a comparison of Figs.6f and 7a.

The oxygen-acetone lignin of **Fig. 8** exhibited micrometer morphology similar to the parent softwood lignin in Fig.5. Higher resolution revealed some difference, however. There was formation of broad filamentous structures instead of wavy aggregates. It was not surprising that sodium lignosulfonate, which differs in its chemical structure from other lignins, also demonstrated characteristic differences. Figure 8 shows these occurred at micrometer and nanometer levels. More surprising is that both humic and fulvic acid images on muscovite were very similar to the images of both pulping and milled wood lignins (**Fig. 9**). Examination of the fractal dimensions in Table I and the cross sections also shows such similarity.

DISCUSSION

Scanning electron microscopical observations of both wood and pulping lignins at a micrometer scale revealed spherical particles comparable in size and shape *(13-18)*. These are consistent with the view of lignin as a statistical polymer in which molecules may form aggregates by physical linkages *(2)*. Aggregates of globular particles

are typical of lignins,and their intrinsic properties were thought to determine their morphologies *(2, 13)*. Morphological similarity between chemically distant native and pulping lignins would not be surprising,if the major chemical process determining lignin solubilization during the pulping process is functionalization and not merely depolymerization *(36)*. Transmission electron microscopy has revealed similar structures in soil fulvic and humic acids deposited on mica *(19)*. Some data has also suggested that the structure of a polymer and the sample preparation technique determine the observed morphology *(16)*. This is why it was so important for comparison purposes to apply alternative experimental techniques to both the lignins and related compounds.

One may consider low molecular weight aromatic molecules as chemical models of lignin, DHP of coniferyl and related alcohols as polymeric models, and pulping lignins as chemical derivatives. The results of our chemical experiments in Fig. 1 and literature analysis *(9)* prove the inclusion of soil humic substances *(37)* into the series of lignin chemical derivatives.The treatment with dry hydrogen iodide is a highly selective procedure that splits ester bonds and b-aryletheric bonds in benzyl alcoholic but not benzyl keto structures *(33)*. Absence of monomeric products of splitting in humic substances (unlike lignins) is not surprising because humic substances are deeply oxidized forms of lignin *(9, 37)*. Reductive depolymerization of humic substances yields significant amounts of trimeric products that are residues of branching knots in a lignin network. This suggests some preservation of topological structures and characteristic lignin interunit bonds during biotransformation of plant residues in the environment. Other methods

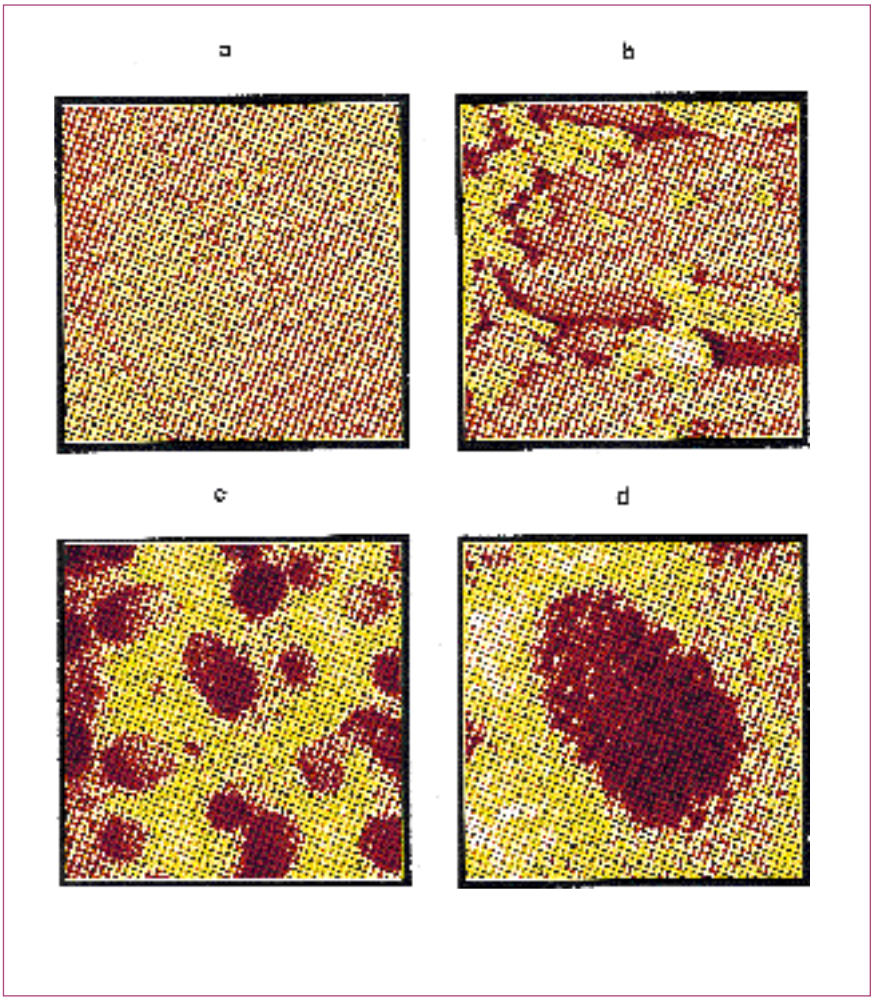

5. Images of spruce milled wood lignin deposited from dioxane for STM on graphite:a. 5 x 5 µm, height 0–45 nm; b. 400 x 400 nm, height 0–20 nm and AFM on muscovite: c. 3 x 3 µm, height 0–30 nm; d. 1.25 x 1.25 µm, height 0–20 nm

also demonstrate striking similarities between lignins and humic substances in their topological (fractal dimension) *(38, 39)* and supramolecular (shape in the solution) *(40, 41)* characteristics.

The micrometer-scale images obtained by scanning probe microscopy differed from those observed by electron microscopy and were substrate-dependent. This study used two standard substrates—graphite and muscovite. These form nearly-ideal flat surfaces when properly cleaved.Graphite has an almost-ideal "van der Waals surface." One should determine morphology of polar molecules on graphite mostly by the inter-aggregate interactions. Muscovite, however, is an aluminosilicate with its basal surface formed by hexagonally arranged oxygen atoms *(42)*. Strong polar interactions with hydroxyl containing polymers involving formation of numerous hydrogen bonds might occur then. The interactions between lignins and muscovite resemble their interactions with kaolinite.This influences the properties of both residual lignin in paper and lignosulfonates in commercial

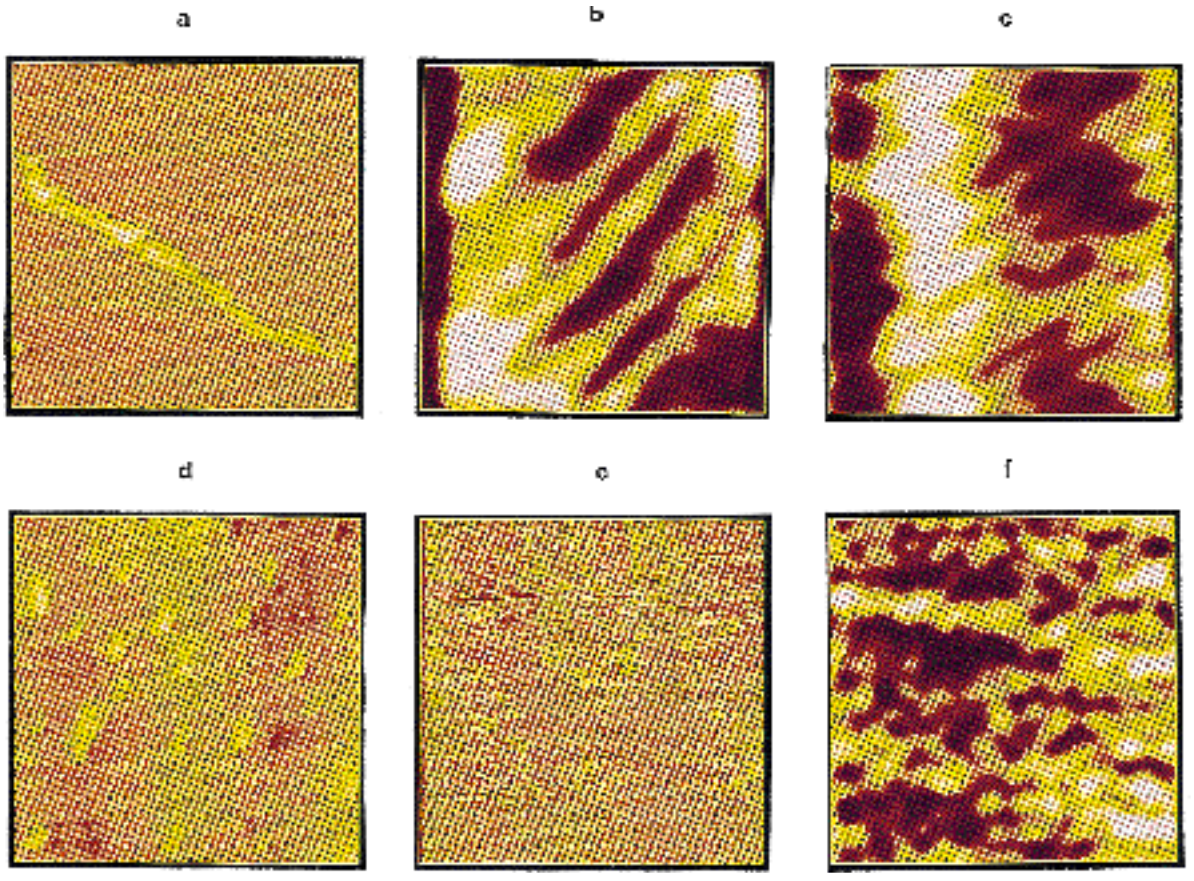

6. AFM images of birch milled wood lignin deposited from dioxane on graphite:a. 3 x 3 µm, height 0–150 nm; b. 20 x 20 nm, height 0–0.5 nm; c. 3 x 3 nm, height 0–0.4 nm; on muscovite:d. 3 x 3 µm, height 0–25 nm; and of eucalyptus dioxane lignin deposited from dioxane on graphite: e. 3 x 3 µm, height 0–14 nm; f. 2.5 x 2.5 nm, height 0–0.6 nm

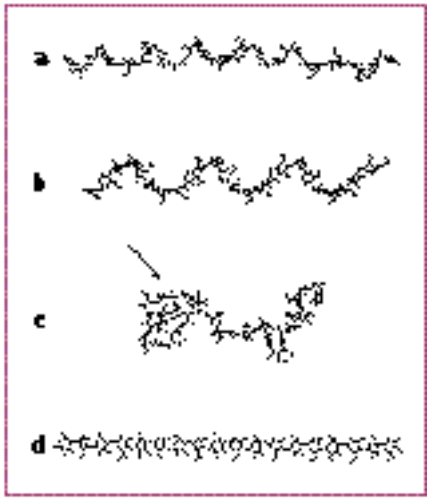

7. Computer simulation of linear chains in lignin (guaiacyl units): a. regular extended helix, b. regular flexible helix, c. irregular conformer with a regular part marked with an arrow, and d. cellulose (ribbon, ß-D-glucopyranose units)

applications *(43)*. The organic polymers on the muscovite surface are also a good model for lignins and related humic substances deposited on mineral surfaces in soil *(44)*.

Figures 4–6 compared to earlier published electron microscopic images clearly demonstrate the effect of sample preparation and substrate surface on the micrometer morphology. They do not confirm regular spherical particles as typical of both lignins and the products of their chemical transformation. One can sometimes observe spherical particles but not necessarily always. On graphite, a large portion of aggregates (spruce MWL: 30–150 nm width, 2–10 nm height; birch MWL: 300 nm–2 µm width, 10–50 nm height) reside along a graphite defect area. This is due to imperfect cleavage resulting in oxygenation of graphite edges that therefore attract polar molecules. Figures 3–6,8,and 9

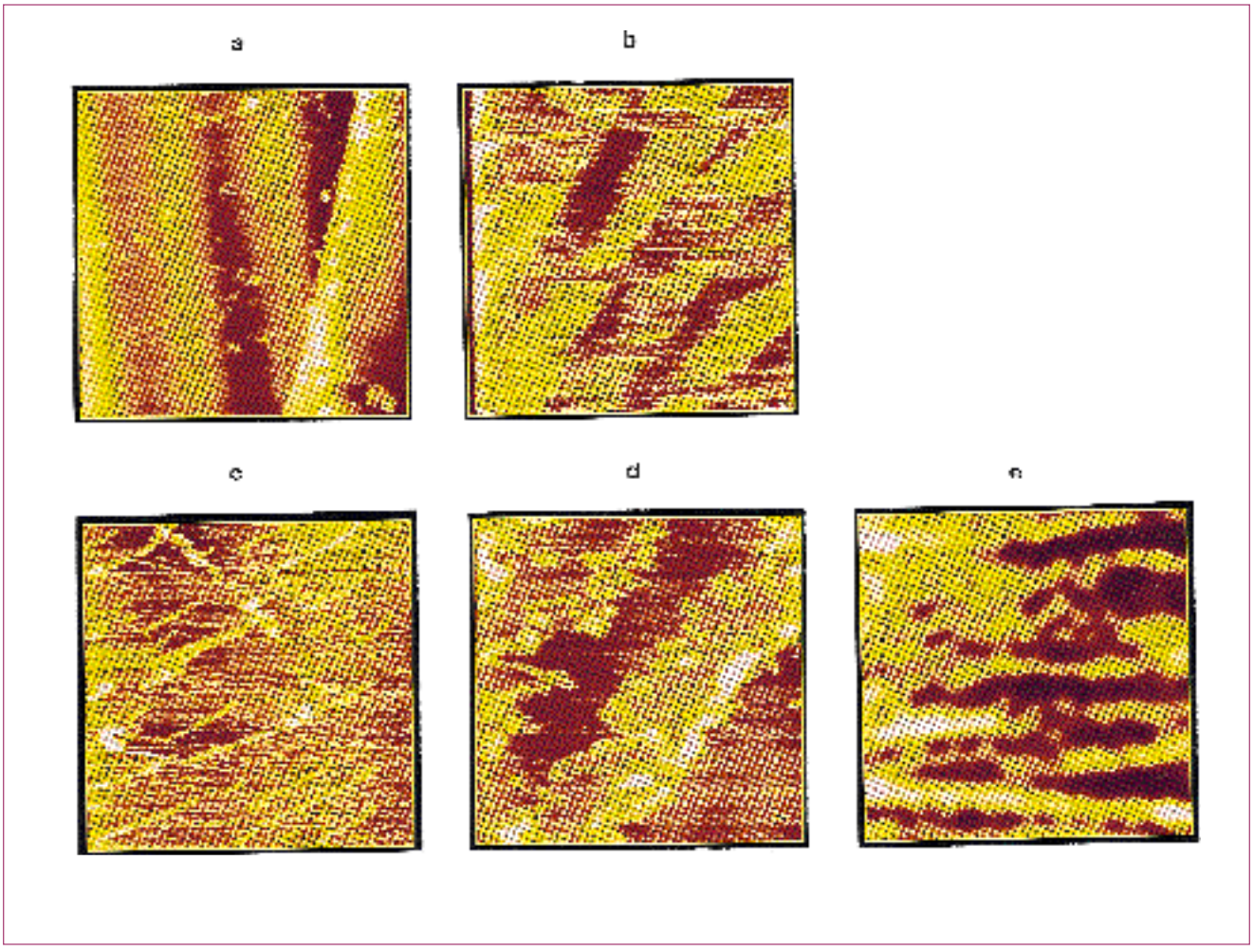

8. AFM images of technical lignins from spruce wood on graphite for oxygen-acetone lignin deposited from dioxane: a. 5 x 5 μm, height 0–47 nm; b. 900 x 900 nm, height 0–8 nm and sodium lignosulfonate deposited from water: c. 10 x 10 μm, height 0–250 nm; d. 3 x 3 μm, height 0–30 nm; e. 2 x 2 nm, height 0–0.3 nm

show that wavy and filamentous structures are also usually present. One can also observe a pronounced effect of the mineral polyoxygen surface on the micrometer morphology in the images of lignins and a model DHP. Figures 4–6 show this.In wood itself, polar cellulose fibers affect lignin morphology. Compare Figs. 5 and 6 to see that the chemical nature of a lignin-related compound is important.Our results suggest, however, that actual morphology and chemical behavior of lignins and related polymers under pulping and environmental conditions receives strong influence from surrounding polar matrices. This may be either organic or inorganic. The properties of the isolated polymers do not entirely predict this.

Micrometer-scale morphology of low molecular weight lignin model compounds, DHP, and lignins on graphite is often identical. This reflects similarity in chemical structure. In turn, this provides similar ways of aggregation in the zones of surface imperfections.It is characteristic that surface properties of sodium lignosulfonate differ significantly from the properties of other lignin-related compounds. On muscovite, soil humic and fulvic acids from Fig. 9 form structures resembling those of lignins as in Figs.5 and 6.One may assume that similarities in the primary structure between the two classes of compounds result in similarities of aggregates formed by macromolecules on the basal polyoxygen mineral surface.

Nanometer-scale morphology always demonstrated general similarity in molecular packing and fractal dimension as Table I indicates.Interpretation of the images of low molecular weight lignin model com-

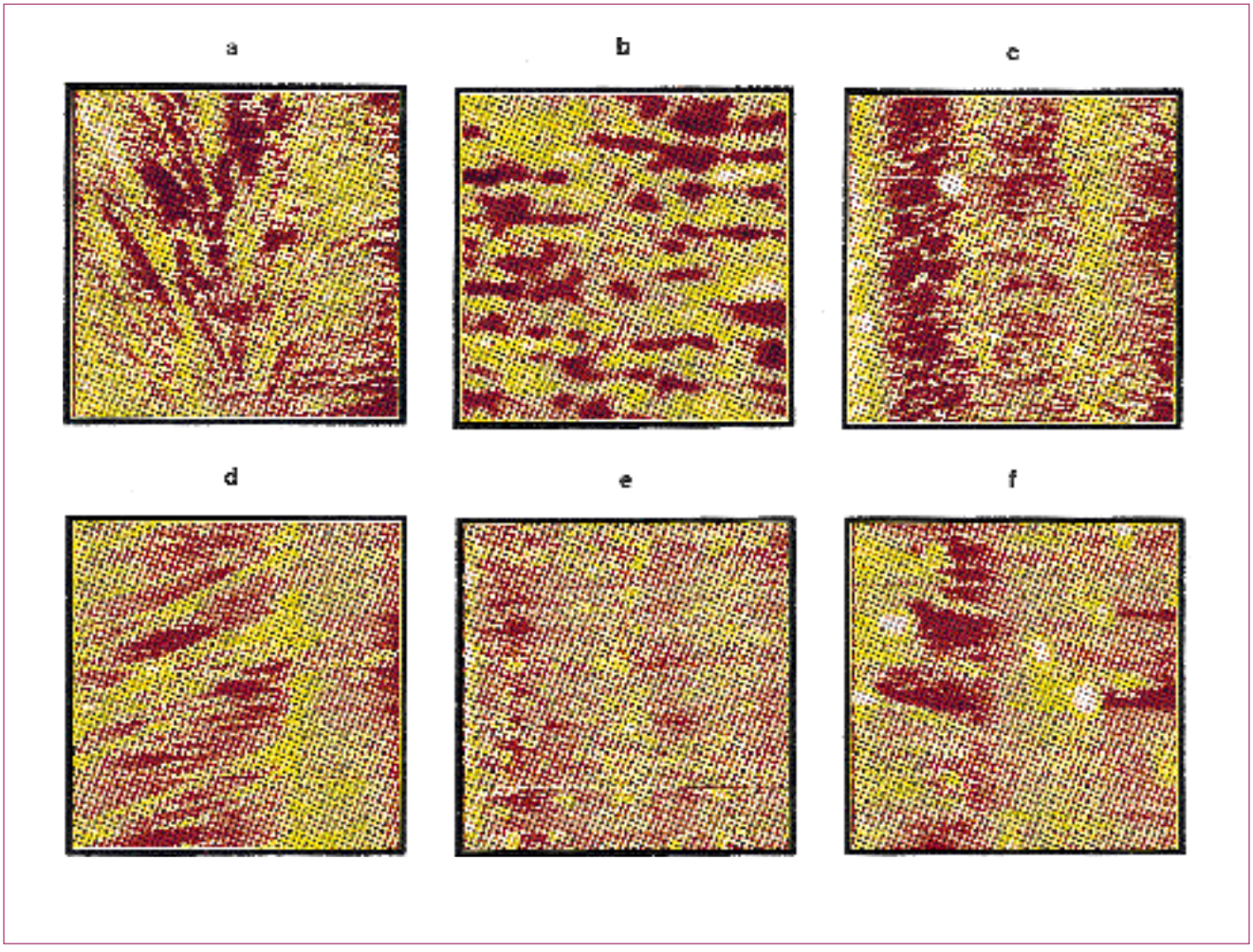

9. AFM images of humic materials deposited from water on muscovite for Suwannee River fulvic acid: a. 2 x 2 μm, height 0–18 nm; b. 4 x 4 nm, height 0–0.8 nm; for Suwannee River humic acid: c. 6 x 6 μm, height 0–60 nm; d. 1.5 x 1.5 μm, height 0–40 nm; and for Canadian soil fulvic acid: e. 4 x 4 μm, height 0–100 nm; and f. 50 x 50 nm

pounds is possible using molecular mechanics simulation. Figure 3c gives an example. The simulated aggregate corresponded closely to the experimental image. It may provide a conceptual picture for the spatial arrangement of individual molecules in the aggregate and the morphology of an irregular surface of a lignin-related compound in a solid state.The nanometer morphology of DHP on two entirely different surfaces—graphite and muscovite—is similar. It is also very similar to the morphology of both model compounds and humic substances. This characteristic reflects the fact that lignin-related polymers coating the inorganic surface usually form multiple layers. Here contiguous layers but not the underlying structure affect the spatial organization of structural units. General similarity here implies that the spatial organization of polymer units may resemble that in the simulated aggregate of a low molecular weight model compound in Fig.3c.It is also important to note, however, that this does not always occur. This is because the polymeric nature of compounds under consideration may result in spatial organizations different from those in a random aggregate of small molecules where chemical bonds do not connect "structural units." The usual values of fractal dimension of Table I that reflect general uniformity in roughness and interunit distances in all studied aggregates therefore characterize birch MWL and sodium lignosulfonate images in Figs. 6c and 8e. They also reveal unusual filamentous structures.

For birch lignin in Fig. 6, linear parts of lignin chains apparently appeared. Earlier investigation reported molecular mechanics cal-

KEYWORDS
Anatomy, bibliographies, humic materials, lignins, microscopy.

culations showing that the lowest energy conformation of a lignin macromolecule is a flexible, broad helix with intercoil chemical linkages *(30)*. Our preliminary molecular mechanics calculations support the idea of two basic types of helixes characteristic of linear chains in lignin. Figure 7a shows an extended one with 1.0-nm diameter and 1.2-nm period, and Figure 7b shows a flexible one with 1.3-nm diameter and 2.3-nm period.Substitution of a guaiacyl unit for a syringyl one does not affect basic geometrical features. Molecular dynamics calculations have shown that a series of thermal conformational transitions may result in low-energy irregular conformers with regular parts. Figure 7c presents an example of such a structure.Its regular part marked with an arrow in the figure with 1.5-nm diameter and 0.5-nm period corresponds closely to the image in Fig. 6c. It has apparent diameter of approximately 1.5 nm and an approximate period of 0.5 nm. A superposition of extended lignin helixes may produce the surface image similar to that of eucalyptus lignin of Fig. 6f provided mostly "upper"parts of the helixes appear. For comparison, Fig. 7d presents an extended ribbon conformer that results from the simulation of cellulose.

CONCLUSION

This report is one of the first dealing with AFM and STM applied to materials of interest in the pulp and paper industry. It may also be the first to use molecular mechanics simulation for interpretation. The reader must therefore consider our conclusions as preliminary. We offer our examples to display the concepts and techniques for future application.Even this initial application, however, achieved excellent nanometer-scale resolution images. There is a limitation to soluble samples so far. This suggests the technique can provide a better understanding of the surface properties of lignin-related compounds, their differences and similarities, and their behavior in industrial and ecological processes.This comparative study of lignin in living plants, pulping lignins,and humic substances in soil is also a necessary step on the way to potential acceptance and use of waste lignins in agriculture and silviculture.

The use of AFM and STM made it possible to obtain micrometer- and nanometer-scale images of lignins, lignin model compounds,and humic substances on nonpolar and polar substrates. Our study has revealed a variety of morphologies affected by chemical structure and polymeric properties of the samples and substrate characteristics and sample preparation procedure. Underlying polar surfaces characteristic of soil inorganic components and coating agents in paper proved to influence strongly the surface properties of lignins and related polymers.Chemical and morphological similarities between lignins and humic substances of soil suggest the use of some waste lignins as pollutant traps and soil improvement agents in the environment. **TJ**

Shevchenko is NRC senior research associate, Akim is NRC research associate, and Bailey is research soil physical chemist at U.S. Environmental Protection Agency, 960 College Station Rd.,Athens, GA 30605. Yu is research chemist/engineer at Technology Applications, Inc.,at the same address.

The authors thank K.-E.L.Eriksson and J.F.D. Dean for kindly supplying a sample of coniferyl alcohol DHP, D. Evtuguin for a sample of oxygen-acetone lignin, C. Pascoal Neto for a sample of eucalyptus lignin,J. P. Simon for helpful discussions on conformational analysis of lignin, and A. Gandini for providing experimental facilities in the HI splitting experiments. Funding for this research came partly from U.S. Environmental Protection Agency Contract No. 68-C1-0024 to Technology Applications, Inc. and from the National Research Council.

Received for review March 3,1995.

Accepted May 9,1995.

LITERATURE CITED

1. Côté,W. A., *Wood Sci. Tech.* 15:1(1981).
2. Fengel, D. and Wegener, G., *Wood (Chemistry, Ultrastructure, Reactions),* de Gruyter, Berlin,1984.
3. Hansma, P. K.,Elings,V. B.,Marti, O., *et al., Science* 242:209(1988).
4. Radmacher, M.,Tillmann, R. W., Fritz, M., *et al.,Science* 257:1900(1992).
5. Sarid, D., *Scanning Force Microscopy,* Oxford University Press, New York, 1994.
6. Doro Pereira,D. E.and Claudiod-da-Silva,E., *Proceedings of the 8th International Symposium on Wood and Lignin Chemistry,* Helsinki, 1995, v.1, p. 467.
7. Hanley,S.J.and Gray, D. G., *Holzforschung* 48: 29(1994).
8. Radotic, K.,Simic-Krstic, J., Jeremic, M., *et al., Biophys. J.* 66:1763(1994).
9. Shevchenko, S. M. and Bailey, G. W., *Critical Rev. Envir. Sci. Tech.,* in press.
10. Haider, K., *Soil Biochem.* 7:55(1992).
11. Kögel-Knabner, I., *Soil Biochem.* 8:101(1993).
12. Kosikova, B., Joniak, D., Hricovini, M., *et al.,Holzforschung* 47:116(1993).
13. Mlynar, J., Kosikova, B., Zakutna,L., *et al., Cellulose Chem. Technol.* 24:475(1990).
14. Fengel, D., *Holzforschung* 30:1(1976).
15. Fengel, D.,Wegener, G,and Feckl,J., *Holzforschung* 35:111(1981).
16. Karmanov, A. P., Fillipov, V. N., and Moskvicheva, T. V., *Wood Chemistry* 1–3: 123(1993).
17. Kallavus, U. and Gravitis, J., *Wood Chemistry* 6:98(1987).

18. Wegener, G. and Fengel, D., *Tappi* 62(3):97(1979).
19. Stevenson,L.L.and Schnitzer, M., *Soil Science* 133:179(1982).
20. Shevchenko, S.M.,Jakobsons,J.,Mishnev, A. F., *et al., Zhurn. Strukt. Khim.* 30(5):135(1989).
21. Stomberg,R.and Lundquist,K., *Nordic Pulp Paper Res. J.* 9(1):37(1994).
22. Shevchenko, S.M., in *Advances in Oxygenated Processes* (A. L. Baumstark, Ed.), JAI Press,Greenwich, 1995, V. 4, pp. 131-175.
23. Björkman,A., *Svensk Papperstidn.* 59: 477(1956).
24. Pepper, J. M. and Wood, P.D.S., *Can. J. Chem.* 40:1026(1962).
25. Zarubin,M.Ya.,Deineko, I. P.,Evtuguin, D., *et al., Tappi J.* 72(11):163(1989).
26. Weymouth,N., Dean,J.F.D.,Eriksson, K.-E.L., *et al., Nordic Pulp Paper Res. J.* 8(4):344(1993).
27. Clark, M., Cramer, R. D., and Van Opdenbosch, N., *J. Computat. Chem.* 10:982(1989).
28. Gasteiger, J., and Marsili, M., *Tetrahedron* 36:3219(1980).
29. Purcel, W. P. and Singer, J.A., *J. Chem. Eng.Data* 12:235(1967).
30. Faulon,J.-L.and Hatcher, P. G., *Energy and Fuels* 8:402(1994).
31. Simon, J.P. and Erikkson,K.-E.L., *Holzforschung* 49:429(1995).
32. Akim, L. G., Shevchenko, S. M., and Zarubin, M. Ya., *Wood Sci. Tech.* 27: 241(1993).
33. Shevchenko, S. M., Akim, L. G., and Zarubin, M. Ya., *Tappi J.* 74(4): 257(1991).
34. Shevchenko, S. M., Akim, L. G., Tanahashi, M., *et al., J. Wood Chem. Tech.,* 15(2):163(1995).
35. Mandelbrot,B.B., *The Fractal Geometry of Nature,* Freeman, San Francisco, 1983.
36. Evstigneyev, E., Maiyorova, H., and Platonow, A., *Tappi J.* 75(5):177(1992).
37. Stevenson, F. J., *Humus Chemistry: Genesis, Composition, Reactions,* 2nd edn., Wiley, New York,1994.
38. Rice, J.A.and Lin,J.-S., *Environ.Sci.Tech.* 27:413(1993).
39. Karmanov, A. P. and Monakov, Yu. B., *Wood Chemistry,* 2:34(1994).
40. Barak, P. and Chen, Y., *Soil Science* 154: 184(1992).
41. Monakov,Yu.B.,Belyaev,V.Yu.,and Karmanov, A. P., *Doklady RAN* 333(2): 200(1993).
42. Bailey, S. W., *Rev. Mineralogy* 13: 13(1987).
43. Afanasiev, N. I., Telysheva, G. M., Makarevich, N.A., *et al., Wood Chemistry* 2:85(1990).
44. Sposito, G., *The Surface Chemistry of Soils,* Oxford University Press, New York,1984.